



Long discharges in a steady state with D₂ and N₂ on the actively cooled tungsten upper divertor in WEST

T. Loarer¹, T. Dittmar² , E. Tsitrone¹, R. Bisson³, C. Bourdelle¹, S. Brezinsek² , J. Bucalossi¹, Y. Corre¹, L. Delpech¹, C. Desgranges¹, G. De Temmerman⁴, D. Douai¹, A. Ekedahl¹, N. Fedorczak¹, A. Gallo¹, J. Gaspar⁵, J. Gunn¹, M. Houry¹, P. Maget¹, R. Mitteau¹, P. Moreau¹ and WEST team^a

¹ CEA IRFM, F-13108, St Paul Lez Durance, France

² Forschungszentrum Jülich GmbH, Institut für Energie und Klimaforschung – Plasmaphysik, 52425, Jülich, Germany

³ Aix-Marseille University, CNRS, PIIM, Marseille, France

⁴ ITER Organization Route de Vinon-sur-Verdon, CS 90 046, 13067, St. Paul Lez Durance Cedex, France

⁵ Aix Marseille University, CNRS, IUSTI, Marseille, France

E-mail: thierry.loarer@cea.fr

Received 17 July 2020, revised 11 September 2020

Accepted for publication 16 September 2020

Published 29 October 2020



CrossMark

Abstract

Nitrogen (N₂) will be used in ITER to enhance the radiative fraction to ~90%, thereby cooling the edge plasma and preventing damage to the plasma-facing components. However, the reactivity of N₂ with hydrogen isotopes can lead to the formation of tritiated ammonia (NT₃). This should be considered in terms of the in-vessel tritium inventory, the regeneration of the cryo pumps, and the processes in the ITER de-tritiation plant. In the ‘W’ Environment in Steady-state Tokamak (WEST), a series of long L-mode discharges (~50 s), with a constant N₂ seeding from the outer strike point region has been performed on the upper actively cooled divertor. In the absence of active pumping, the N₂ balance shows steady-state retention during plasma discharge, and is partially (~35%) released in between discharges. Although a significant amount of N₂ (18.65 Pa m³) has been injected, the wall still exhibited N₂ pumping capabilities. Under these conditions, as long as this N₂ reservoir is not saturated, there is not enough N available for the detectable threshold of ND₃ formation to be reached. In these WEST experiments, no ammonia is detected during the pulse or after the pulse in the outgassing phase. These results are consistent with and complementary to the N₂ seeded experiments performed in the Joint European Torus (JET) with its ITER-like wall and in the Axially Symmetric Divertor Experiment (ASDEX) upgrade.

Keywords: WEST, long pulses, steady state, plasma surface interaction, nitrogen seeding, ammonia

(Some figures may appear in colour only in the online journal)

1. Introduction

Heat load control on plasma-facing components (PFCs) is a critical issue in magnetically confined fusion devices. The

plans for the operation of ITER and DEMO will rely on the injection of low-Z impurities, potentially improving plasma confinement, but particularly for reducing the heat loads on the PFCs via enhanced radiation in the edge plasma. Indeed, the current design, based on the technologically achievable level given the materials to be used in ITER, is in

^a See <http://west.cea.fr/WESTteam>

the range of 10 MW m^{-2} , in steady state and transiently 20 MW m^{-2} [1, 2]. Without this enhanced edge radiation, the heat flux at the divertor strike point is expected to reach ranges $>50 \text{ MW m}^{-2}$, far above the acceptable power threshold of the PFCs. Using carbon-based PFCs, a high carbon concentration was achieved in the edge plasma through erosion and transport by the edge plasma, leading to high radiation in the vicinity of the divertor targets. With fully metallic PFCs, such as the full-tungsten Axially Symmetric Divertor Experiment (ASDEX) upgrade (AUG), the Joint European Torus (JET) with its ITER-like wall (JET-ILW), and to a greater extent ITER and DEMO, the intrinsic concentration of low-Z impurities is significantly lower. Therefore, low-Z impurities require to be introduced into the edge plasma as seeded gases [3], to dissipate a sufficiently high fraction of the energy entering the scrape-off layer (SOL), in order to reduce and to control the divertor heat loads. So far, most of the investigations into the highly radiative plasma scenario in metallic fusion devices have been focused on argon, neon and nitrogen, with a few being performed with krypton and xenon [3]. In this context, compared with the carbon environment, nitrogen seeding has allowed for similar plasma performances [4], due to the very close radiative performances of N and C.

However, the potential reactivity of N_2 with hydrogen isotopes can lead to the formation of tritiated ammonia (NT_3) as well as ND_x and NT_y , which should be considered for the regeneration of cryo pumps and processes in de-tritiation plants. In ITER, the tritium plant needs to decompose ammonia to recover the tritium since, for reasons of safety, a maximum of 180 g is allowed in the cryopumps. In addition, the potential formation of nitrogen oxides should also be avoided in the high-temperature process required for NT_3 recovery [1].

Moreover, the activation of these low-Z seeding gases (argon, krypton, neon, nitrogen and xenon) in nuclear environments is another issue which is often neglected. Although not discussed in this work, the consequences of the potential activation of these gases and their respective progenies as a result of the neutron flux generated during deuterium—tritium (DT) operations are reported in [5] for DEMO scenarios.

The quantification of the ammonia formation via surface reactions between nitrogen and hydrogenic species on PFCs has yet to be completed. At this stage, it is not yet possible to predict the ammonia formation rates expected in the different ITER plasma scenarios [2]. However, the use of N_2 as a radiator in the edge plasma, particularly in the divertor, in the ITER facility is still nevertheless considered as a viable seeding candidate for the size and conditions of present-day PFCs, in particular the divertor.

The work reported in this paper concentrates on N_2 injection, and the potential formation of ammonia (ND_3). The objective of the reported experiments is to study the pumping behaviour of N_2 with metallic PFCs and the formation of ammonia due to N_2 injection during long discharges.

The tokamak formerly known as Tore Supra, initially designed for long-pulse operation, has recently been modified to become the W Environment in Steady-state Tokamak (WEST) [6, 7], changing from a limited to a diverted magnetic configuration, and from carbon to tungsten PFCs. The

aim of this project is to test the ITER divertor technology via long discharges for material behaviour studies, to assess the consequences of high fluences on tungsten PFCs, and also to examine the corresponding effects on plasma performances. In this context, a series of steady-state long pulses with N_2 seeding is carried out in WEST to assess the N_2 particle balance and the potential ammonia formation in a fully actively cooled tungsten device. The objectives here are to improve the understanding of the physics of the ammonia production, its decomposition and transport in a magnetically confined plasma device. In this study, the overall N_2 particle balance is evaluated based on the long discharge configuration and the steady-state capabilities of WEST, using the actively cooled upper divertor. These experiments are therefore complementary to those already carried out at both JET-ILW and AUG [8, 9], with inertial PFCs leading to high surface temperatures and limited plasma durations in the range of 6–7 s.

For the reported configuration, in its ‘phase 1’, WEST is [6] equipped with a mix of ITER-like actively cooled PFUs (bulk W designed for a heat flux of up to 20 MW m^{-2}) and non-actively cooled W-coated graphite components (W-coating $\sim 20 \mu\text{m}$ thick) in the lower divertor. The upper divertor is fully equipped with actively cooled copper-based PFCs, coated with $\sim 20 \mu\text{m}$ of tungsten, allowing long discharges in steady-state conditions. In the upper single null (USN) configuration, a heat flux of up to 8 MW m^{-2} and/or a total heat removal capability of 5 MW in the steady state can be achieved. Although no active pumping has been installed in the upper divertor, long discharges are now routinely performed using the USN configuration [10]. In this study, five repetitive long deuterium (D_2) discharges in the range of 50 s in a steady state are performed in the USN configuration, with a constant N_2 injection for up to 35 s from the outer strike point region (OSP), in order to assess the N_2 particle balance and the resulting potential ND_3 formation.

In the first section, the experimental context and the main plasma parameters are reported, based on the main diagnostic measurements from the Langmuir probes, bolometry, VIS, UV spectroscopy and mass spectrometry. In the second section, the particle balance for both D_2 and N_2 is described, to complement the monitoring of the ND_3 during the plasma and the recovery phases. The final section is dedicated to the discussion of these results and their comparison with those obtained from JET-ILW [8] and AUG [9].

2. Plasma experiments

The reported series of experiments was performed after 40 pulses, subsequent to boronisation. These 40 plasma pulses amounted to an overall duration of 452 s, comprising 30 pulses (for a total of 166 s) in the lower single null (LSN) configuration, and ten long discharges (for a total of 286 s) in the USN. Of these 40 discharges, 25 were run with lower hybrid (LH) auxiliary heating, P_{LH} , ranging from 1.0 to 4.4 MW. In this context, the potential effects of boronisation (performed with 10% diborane (B_2D_6) and 90% Helium using a glow discharge) on the plasma were considered to be negligible, both in terms of recycling and impurity content. This was also

supported by the ten repetitive discharges performed in USN (without N_2 injection) prior to these experiments, including a discharge (#55 786) in USN with 3.0 MW of LH heating (P_{LH}) for 55 s. All these repetitive discharges exhibited the same main parameters (density, radiated power, etc.) in the first few seconds (~ 0 –3 s) of the plasma discharge, as well as during the different heating phases, while the level of oxygen remained within the range observed prior to boronisation.

For these experiments, the main parameters were a plasma current, I_p , of 400 kA, a toroidal field, B_T , of 3.7 T, a P_{LH} of 3.0 MW, a line integrated plasma density, n_l , of $3.3 \times 10^{19} \text{ m}^{-2}$ in L-mode and USN configuration. In this plasma configuration, there was no active pumping in the sub-divertor region controlling the plasma density or the N_2 plasma content. The only pumping system for these experiments was the ‘maintenance’ system (turbo pumps) ensuring the basic pressure in the vacuum vessel, and the five turbo pumps located on the lower sub-divertor. However, as will be shown, these pumping systems are not at all efficient for particle exhaust during USN plasma operations. This means that all the gas (D_2 and N_2) injected remained in the plasma volume and/or in the wall (through implantation and co-deposition). On the one hand, the absence of active pumping appears to be an operational challenge for both plasma density and radiated fraction control with a constant impurity injection, for durations in the range of 40 s. On the other hand, during the steady-state phase, for a constant plasma density, the gas balance directly exhibits a ‘net’ wall pumping rate for both D_2 and N_2 .

The reported experiments focus on five long discharges (in the ~ 50 s range each), the first of which, with no N_2 injection (#55 787), was used as a reference. For the four following pulses, a constant N_2 seeding was applied from the OSP region. Figure 1 shows a poloidal cross-section of the USN plasma configuration (#55 789 at 15.42 s) with the location of the N_2 injection feed-forwarded at a constant rate in the OSP region. The D_2 was injected through the midplane with a feedback control for achieving a constant density over the entire plasma duration. Table 1 presents a summary of the D_2 and N_2 injection rates and quantities. For these five consecutive and repetitive discharges, the same D_2 injection rate in the range of ~ 0.15 – $0.2 \text{ Pa m}^3 \text{ s}^{-1}$ ($\sim 10^{20} \text{ D s}^{-1}$) has always been required to maintain the plasma density constant over the 50 s of discharge. Figure 2 shows the main plasma parameters (I_p , n_l , P_{LH} , P_{rad} , D_2 and N_2 injection rates) for pulse #55 789 with N_2 seeding, which is representative of this series. After ~ 25 – 30 s, all the plasma parameters were in a steady state and, remarkably, this was the case for all five of these reported discharges.

For the four seeded pulses, the total amount of N_2 injected through the OSP region was 18.65 Pa m^3 . This is a significant amount of N_2 , compared to that used in the experiments reported in [10], where a total of 5.4 Pa m^3 was injected over six pulses for a maximum of 6 s at $0.15 \text{ Pa m}^3 \text{ s}^{-1}$. The highest rate and amount of N_2 were measured for discharge #55 792, in which a total of 9.49 Pa m^3 of D_2 ($4.58 \times 10^{21} \text{ D}$ & $4.58 \times 10^{21} \text{ e}^-$) and 6.32 Pa m^3 of N_2 were injected ($3.1 \times 10^{21} \text{ N}$ & $21.3 \times 10^{21} \text{ e}^-$).

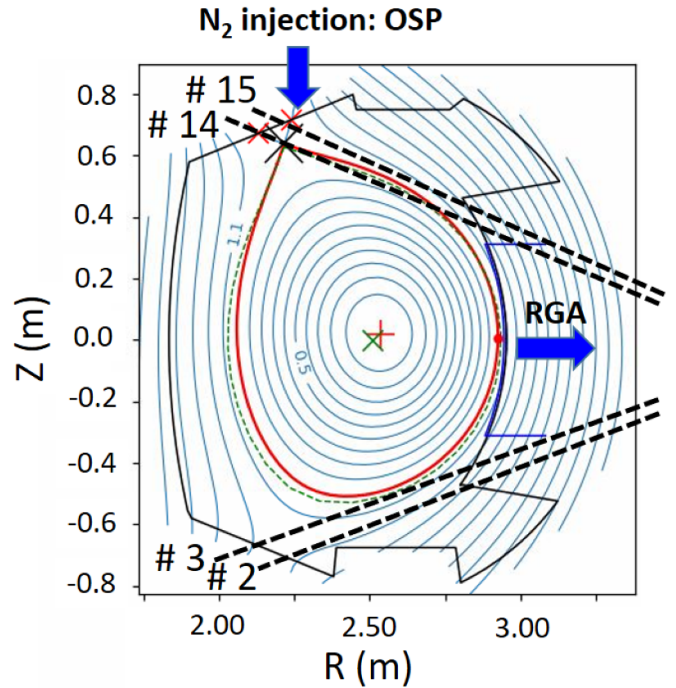


Figure 1. Poloidal cross section of the USN plasma configuration (#55 789 at 15.42 s) with the location of the N_2 injection in the region of the OSP. The residual gas analyser (RGA) used for the gas balance analysis was located in the midplane, whilst the D_2 was also injected through the midplane (using a different port from the RGA) with a feedback control for keeping the density constant over the entire plasma discharge duration. The bolometer tracks probing the edge plasma in the OSP region (#14 and #15) and the lower parts of the plasma (#2 and #3) are also shown.

With the exception of discharge #55 790, N_2 injection was also performed in the early phase of the plasma discharge, from 0 to 3 s. This injection allows for an increase in the edge radiation during the limiter phase and the early X point phase (the X point is formed at 1.0 s), when I_p has reached 300 kA. This procedure enhances the radiation at the plasma edge limiting the W impurity generation while maximising the plasma current profile, temperature, and density. In this phase (from 0 to 3.0 s), the plasma is generally detached, then reattaches during the I_p ramp-up from 300 to 400 kA. However, the amount of N_2 injected during this early plasma phase is negligible, as compared to the injection during the steady state phase (see table 1). In addition, this early and minor N_2 injection has no effect or contribution at all on the plateau phase of the discharge or on the next pulse, as will be shown in the discussion below.

Figure 3 shows a comparison between two consecutive discharges, the first (#55 787) without N_2 , and the second (#55 789) with a constant N_2 injection through the OSP from 10 s to 40 s at $0.1 \text{ Pa m}^3 \text{ s}^{-1}$. No difference can be distinguished in the main plasma parameters between these two discharges. The plasma temperature, T_e , at the OSP region was measured by Langmuir probes located in the upper divertor. Here, T_e is in the range from 5–10 eV in the ohmic phase

Table 1. Summary of the N₂ and D₂ injection and particle balance for this series of long discharges.

Pulse number	#55 787	#55 789	#55 790	#55 792	#55 794
Plasma duration (s)	53	50.5	49	49.6	34.7
N ₂ (0–3 s) Pa m ³	0.134	0.187	0	0.161	0.205
N ₂ inj. rate (Pa m ³ s ⁻¹)/(Ns ⁻¹) (window)	0	0.1/4.8 × 10 ¹⁹ (10–40 s)	0.18/8.7 × 10 ¹⁹ (10–45 s)	0.22/1.1 × 10 ²⁰ (10–45 s)	0.2/9.7 × 10 ¹⁹ (10–35 s)
N ₂ (Pa m ³) injected & (N)	0	2.46 (1.18 × 10 ²¹)	5.48 (2.64 × 10 ²¹)	6.32 (3.05 × 10 ²¹)	4.39 (2.12 × 10 ²¹)
N ₂ (Pa m ³)/pumped (%)	–	0.9/36	2.1/38	2.0/32	3.0/68
D ₂ injected (Pa m ³) (~rate Pa m ³ s ⁻¹)	11.6 (0.2–0.1)	11.6 (0.2–0.1)	11.2 (0.2–0.1)	9.5 (0.2–0.1)	9.76 (0.1)
D ₂ (Pa m ³)/pumped (%)	9.5/82	9.1/78	8.9/179	9.0/94	8.1/83

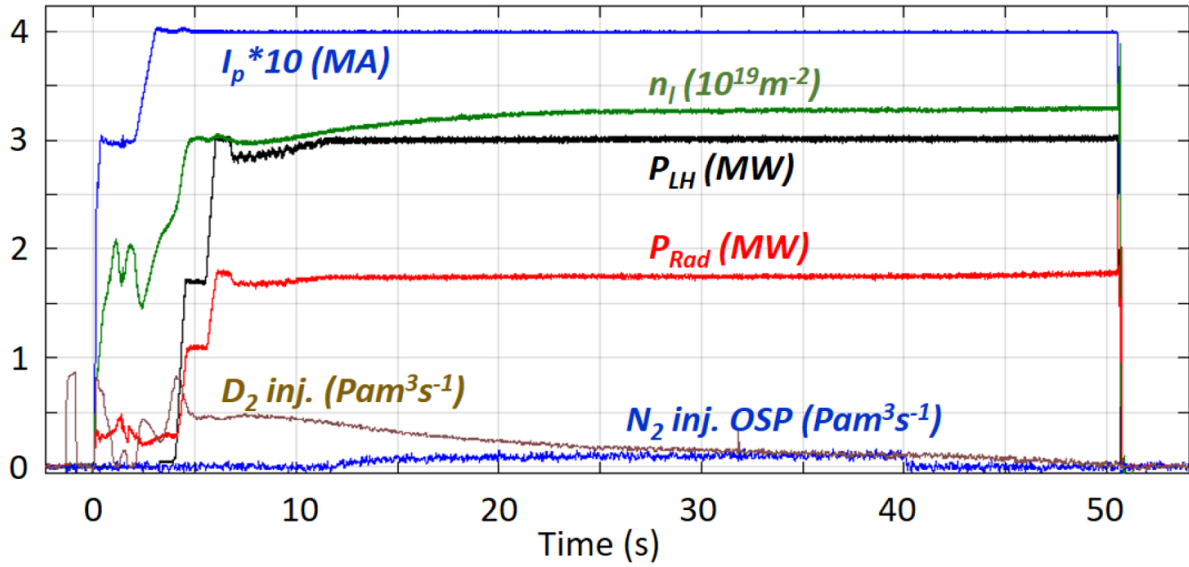


Figure 2. Main plasma parameters: Plasma current, I_p , linear density, n_l , lower hybrid power, P_{LH} , Radiated power, P_{rad} , D_2 and N_2 injection rates for pulse #55 789, which is representative of the series. For all these discharges, a steady state was reached from 25–30 s up to the end of the discharge.

prior to the LH power, increasing to around ~ 15 – 20 eV during the heating phase. Over the entire heating phase, when N_2 was injected, no effect was observed on T_e , which remained in the same range of 15–20 eV. Consistently with these results, the maximum surface temperature in the OSP region was around 300 °C, and this temperature was stable, due to active cooling; no drop, or even variation of the surface temperature, was observed during the N_2 injection. The only effect that was clearly observed was a change in the saturation current measured by the Langmuir probes, which increased by 25% from 4 to 5×10^{-3} A. Furthermore, as the N_2 injection was turned on, the electron flux increased up to a steady state, reverting to its initial value (i.e. that prior to injection) as the seeding was stopped. Several plunges performed with a reciprocating Langmuir probe in similar plasma pulses (see [10]) allowed for both T_e and n_e evaluation, up to a normalised radius of $\rho = r/a \sim 1.05$, showing about $T_e \sim 75$ eV and $n_e \sim 1.6 \times 10^{19} \text{ m}^{-3}$ at the separatrix. Except for a small increase of the density in the SOL during the injection, no effect was observed.

The spectroscopic analysis in the VIS range exhibits an increase of the N(II) signal (at 399.6 nm), as N is injected from discharge to discharge. This effect is more pronounced in the surrounding of the OSP (where N_2 is injected) but this remains a very small effect which stays constant over the injection, showing no accumulation in the vicinity of the edge region and, in particular, close to the location of the main recycling flux. This is confirmed by the bolometry measurements, which indicate that the overall profile of the radiated power is nearly unmodified. Indeed, only the edge tracks of the bolometry exhibit a very minor increase of the signal in the vicinity of the OSP in the course of the N_2 injection. The two tracks probing the edge plasma in the OSP region (#14 and #15—see figure 1) show an increase of $\sim 8\%$ and recover their initial values as the injection is stopped, as illustrated in

figure 4. This effect is not observed for the lower tracks (#2 and #3) viewing the lower part of the plasma and the SOL. This strongly suggests that the extra radiation (although modest) due to the N_2 injection remains only as a ‘local’ effect in the recycling area.

Going deeper into the plasma, the N_2 injection can be weakly observed in the UV range at 247.6 Å for the N(V) signal and at 24.8 Å for the N(VII) signal when averaged over 5 s (from 25–30 s). This is shown in figure 5, where the N(VII) signal at 24.8 Å is plotted as a function of time for discharge #55 792 where the strongest N_2 injection was performed (35 s at $\sim 0.21 \text{ Pa m}^3 \text{ s}^{-1}$). As for the bolometry, a steady state phase was observed for $t > 25$ – 30 s whilst the signal dropped back to its initial value prior to the seeding phase as the injection was stopped. In figure 5, the N(VII) signal at 24.8 Å is plotted as a function of time for discharge #55 790 with no early N_2 injection, showing that the early N(VII) signal peak is not observed, thereby confirming the absence of a potential N_2 legacy from previous N_2 seeding for 30 s at a rate of $0.1 \text{ Pa m}^3 \text{ s}^{-1}$. In the absence of active pumping during the plasma operation, one could have expected a cumulative effect of the N_2 during the discharge (seeding duration of up to 35 s) and also from pulse to pulse. However, no such effect is observed. Based on these experiments, the evidence shows that the injected N_2 enters the bulk plasma only very weakly, whilst being totally dominated by the wall pumping.

Finally, in terms of spectroscopy, no effect can be observed on the other main plasma impurities such as W, O, C, or B. These measurements exhibit a very consistent overview of the very weak effect of the N_2 injection on the radiation pattern (bulk and edge), as confirmed by the Langmuir probes and the IR measurements.

The N_2 balance was monitored by a residual gas analyser (RGA) located in the main pumping duct at the outer mid-plane (see figure 1) of the vacuum vessel. During the plasma

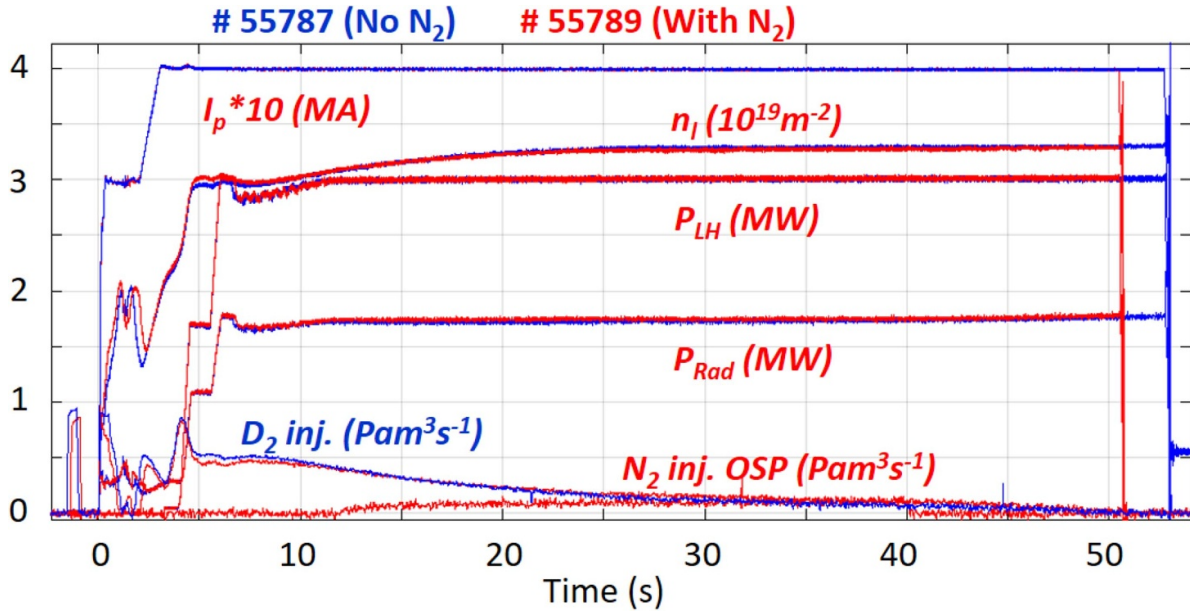


Figure 3. Comparison of the main plasma parameters (I_p , n_l , P_{LH} , P_{rad} , D_2 and N_2 injection rates) for two long discharges without N_2 injection (blue, #55787) and with N_2 injection (red, #55789).

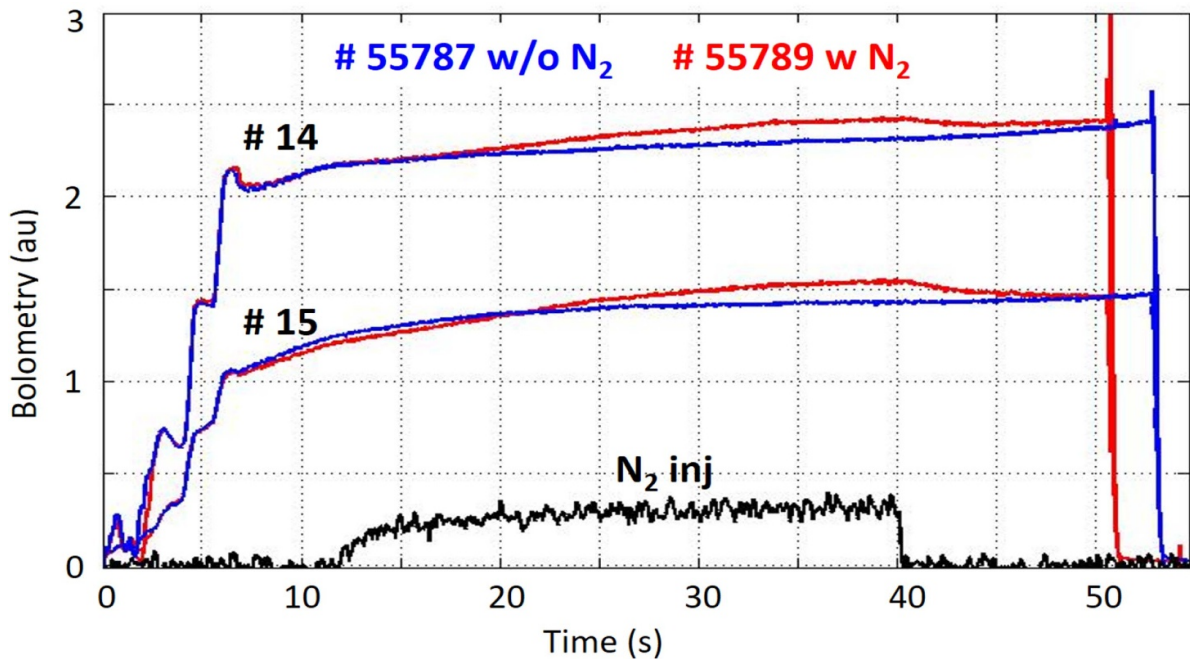


Figure 4. Time evolution of the two upper tracks of the bolometry (#14 and #15—see figure 1) probing the edge plasma in the OSP region for a discharge without N_2 injection (#55787, in blue) and with N_2 injection (#55789, in red). The N_2 injection at $0.1 Pa m^3 s^{-1}$ is shown for pulse #55789. An increase by 8% in the bolometry signal of is only observed on these tracks, but they recover their initial value as the injection is stopped.

operation, the edge-neutral pressure in the midplane was very low, consistently below the 1.0×10^{-3} Pa range for all discharges, and always with D_2 as the dominant species. For all these discharges, the same behaviour of N_2 was observed, more or less independently of the amount injected. Figure 6 shows the time evolution of the mass 28 (N_2), as recorded by the RGA during the plasma and recovery phases for the five discharges of the series; #55787 being run without N_2

injection during the heating phase. This clearly shows that compared to the amount injected, a totally negligible amount of N_2 is pumped through the mid-plane during the pulse; this point is further discussed below. After each pulse, the N_2 recovery increases with respect to the amount injected. However, from pulse to pulse, no real legacy effect can be observed. Indeed, the increase in a mass of 28 can be attributed to the stronger seeding, but no effect is observed during

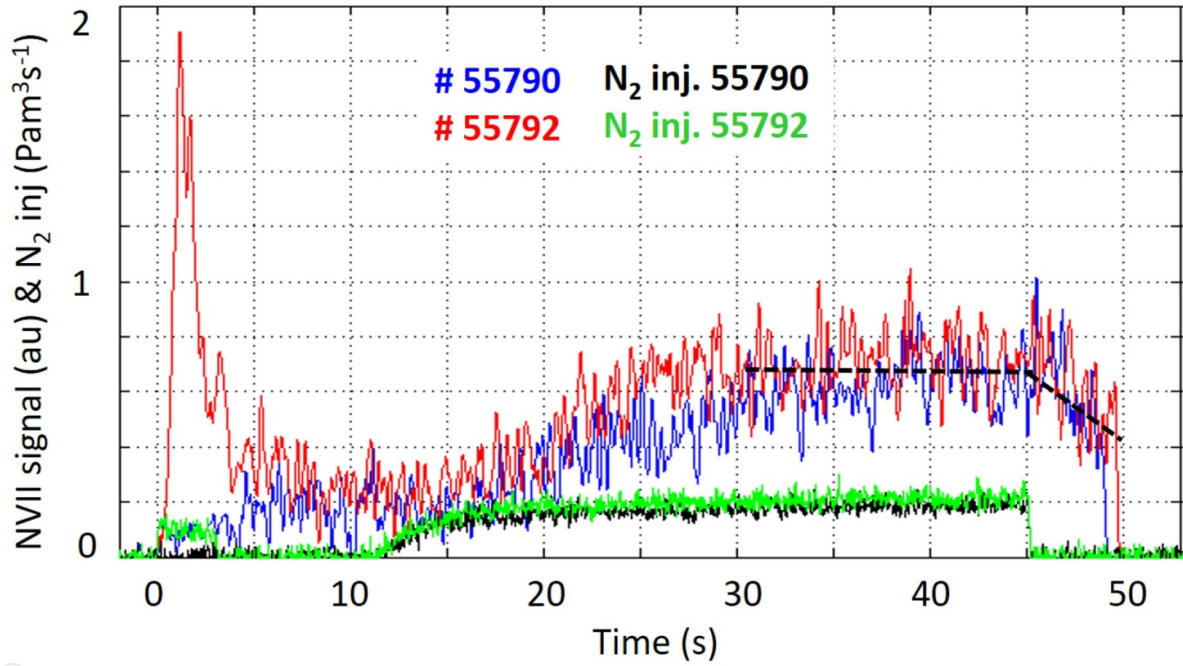


Figure 5. N(VII) signal in the UV range at 24.8 \AA as a function of time for discharges #55 790 (b) and #55 792 (r) and the respective N_2 injection rates (black and green). For pulse #55 790, following the first strong N_2 injection for 30 s (pulse #55 789), no N_2 was injected at the beginning of the discharge. No N(VII) signal was observed in this early plasma phase for the pulse #55790 as opposed to pulse #55 792 where N_2 was injected in the early plasma phase (green signal from 0 to 3 s). The steady-state phase of the N(VII) signal is clearly observed for $t > 30$ s, whereas it drops as the N_2 injection is stopped.

the breakdown and the first few seconds (0–3 s) of plasma, as shown in figure 6. Finally, for the last pulse (#55 794) of this series, strong MHD activity occurred during the heating phase, leading to a disruption during the heating phase. This can explain the higher recovery, due to a different/enhanced plasma wall interaction with the potential N_2 reservoir.

Based on the RGA data, the mass spectra of ammonia overlaps with those of methane and water, which are part of the neutral gas composition in the midplane during both the pulse and post-pulse phases. The model described in detail in [11], allows for the proportion of each of the three gases to be evaluated. This model is the same as that used for both the JET-ILW [8] and AUG [9] N_2 injection and ammonia experiments. For the WEST experiments, the signals of water, methane and ammonia for discharge #55 792 are shown in figure 7. These results clearly indicate that the ND_3 stayed below the detection limit both during the plasma operation and the recovery phase. This is also the case even for discharge #55 792, which contained the most nitrogen, and for the last discharge (#55 794) showing a higher N_2 recovery after the pulse due to the disruption.

During the four discharges, cumulatively totaling more than 3 min of plasma, N_2 was seeded through a toroidal ring located below the upper divertor in the vicinity of the OSP. The nitrogen seeding rate was varied from 0.1 to $0.22 \text{ Pa m}^3 \text{ s}^{-1}$ for a total duration of 125 s to investigate both the potential legacy of N_2 injection on plasma performance and the formation of ND_3 in steady-state conditions. Due to the actively cooled PFCs, the surface temperature reached a maximum of $300 \text{ }^\circ\text{C}$ in steady state. For all these discharges, the main radiative

impurities were identified as W, O, Cu (mainly during the LH power phase) and also including some traces of C. The contribution of N to the overall radiation has always been found to be negligible although N has been observed through both VIS and UV spectroscopy but only during the N_2 seeding phases.

3. Particle balance

The particle balance for the overall vessel at the midplane (and also the RGA location, see figure 1) for both D_2 and N_2 species can be expressed as:

$$\int_0^t \Gamma_{\text{inj}} dt = N_{\text{plasma}} + \int_0^t P S dt + N_{\text{wall}} \quad (1)$$

where Γ_{inj} is the gas injection rate, N_{plasma} is the plasma fuel content, P the neutral pressure close to the pumps at the midplane, S the equivalent pumping speed resulting from the lower divertor pumps and the maintenance pumping system, and N_{wall} is the amount of particles trapped or released by the wall since the start of the plasma at $t = 0$.

This balance can be verified at any time during the plasma discharges for each species (D_2 and N_2) and also after the pulse during the outgassing phase. The total neutral pressure in the vessel, P_{tot} , close to the RGA is measured through a ‘baratron’ type of pressure gauge. Based on the RGA measurements, the composition of the gas released after the pulse is totally dominated by D_2 and N_2 whilst the ‘traces’ of H_2 and H_2O are negligible in the gas balance.

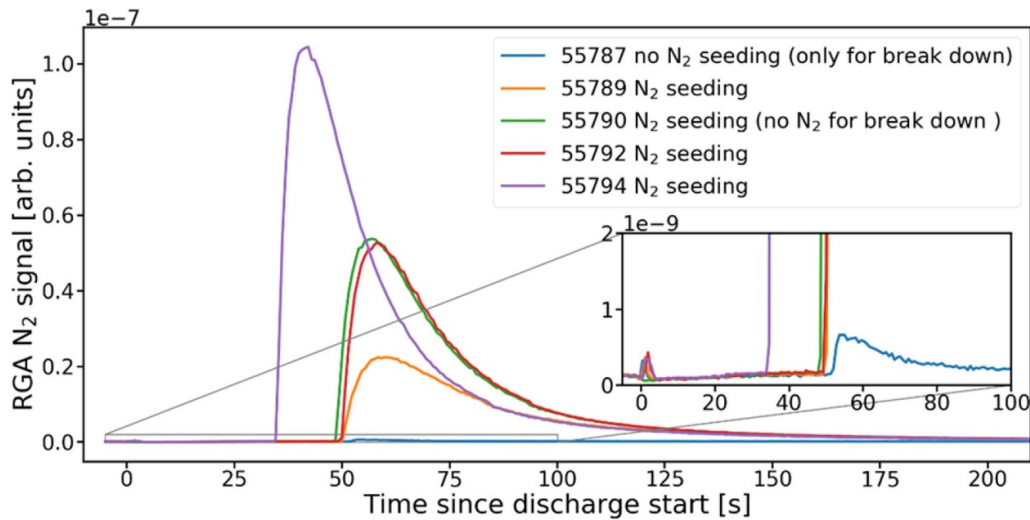


Figure 6. Time evolution of the gas with a mass of 28 (N_2) recorded by the RGA in the midplane for the series of plasma discharges (in the 0 to 50 s range, except for #55 794 which lasted from 0 to 35 s). The increase in the mass 28 signal observed with the increasing discharge number can be attributed to the stronger seeding, but for the last pulse (#55 794) of this series, strong MHD activity occurred that could also explain the higher recovery due to a different/enhanced plasma wall interaction with the potential N_2 reservoir. Insert: zoomed-in time evolution of the mass 28 signal during the plasma discharge and the early phase following the plasma discharge end. This clearly demonstrates that, compared to the recovery phase, a negligible amount of N_2 is pumped during the pulse.

For these experiments in the USN configuration, during the plasma discharge, the neutral pressure in the pumping systems (lower divertor and maintenance) was always lower than $0.5\text{--}1.0 \times 10^{-3}$ Pa. With a total pumping speed of $9.8 \text{ m}^3 \text{ s}^{-1}$ for the D_2 , this led to a maximum pumping rate of $0.01 \text{ Pa m}^3 \text{ s}^{-1}$, smaller by far and negligible compared to the D_2 injection rate which is in the range of $\sim 0.2 \text{ Pa m}^3 \text{ s}^{-1}$. The same conclusion holds true for N_2 since, although very low, no significant increase was measured in the midplane during the plasma discharge. With such a negligible particle exhaust being produced by the pumps, this confirms that for all these discharges, the wall represented the main pump during plasma discharge. Throughout this situation (i.e. without active pumping) in the USN configuration, since the plasma density was constant, this led to a constant retention process of $\sim 0.2 \text{ Pa m}^3 \text{ s}^{-1}$, independently of the accumulated amount of D_2 and N_2 injected in the previous discharges. In these conditions, the particle balance was dominated by the recovery phase following the end of the plasma discharge and can be simply described by equation (1), where $N_{\text{plasma}} = 0$.

Our consideration of the gas balance is focused on a comparison of the reference pulse without N_2 injection (#55 787) and the pulse (#55 792) with the strongest N_2 injection. For pulse #55 787 (with a duration of 53 s), 11.6 Pa m^3 of D_2 was injected, and for pulse #55 792 (with a duration of 49.3 s), 9.49 Pa m^3 of D_2 and 6.32 Pa m^3 of N_2 were injected. Except for the N_2 injected, these two discharges are very similar, both in terms of plasma parameters (I_p , B_T , P_{LH} , nI , and the plasma shape in the USN configuration), duration and D_2 injection rates.

For the pulse without N_2 injection (#55 787), the time evolution of the total neutral pressure in the vessel after the discharge exhibited the usual $\sim t^{-0.7}$ dependence and the extrapolation shows that the initial pressure in the vessel was

recovered after about 30 min. This is illustrated in figure 8, where the time traces of the D_2 pressure and a fit using a function $\propto t^{-0.7}$ are plotted for discharge #55 787. The particle balance shows that 9.5 Pa m^3 of D_2 was pumped that has to be compared with the 11.6 Pa m^3 injected for this discharge.

The particle balance for discharge #55 792 with both D_2 and N_2 injection exhibits a very similar behaviour for the D_2 . Indeed, a total amount of 9.5 Pa m^3 was injected and according to the fit (also using a $t^{-0.7}$ law), the recovery of the initial D_2 vessel pressure occurs at ~ 25 min (See figure 8). Based on this fit, the D_2 balance shows that 9.0 Pa m^3 (94%) was exhausted, which is the highest recovery of the series. For all the other discharges, an average D_2 recovery in a range of $\sim 80\%$ (see table 1) is observed after more than 30 min, which is very consistent compared to what can be expected in a metallic device [8, 9].

The N_2 pressure and the associated balance for pulse #55 792 show that the total N_2 recovered after 25 min was 2.0 Pa m^3 , corresponding to 32% of the total N_2 injected. From these experiments, a different time dependence for D_2 and N_2 pressure in the recovery phase can be observed. Indeed, as shown by the insert in figure 8, the maximum pressure of D_2 is reached at 53 s (the end of pulse was at 49.3 s) whilst the maximum N_2 pressure was observed later, at 58 s. Also, the fit for the partial pressure of N_2 has had to be adjusted by a $t^{-1.6}$ law, suggesting a different outgassing process from the D_2 . In these conditions, about 700 s after the end of the pulse, the N_2 pressure has recovered values that are very close to the values present prior to the pulse. In these experiments, the temperature of the actively cooled PFCs returned to the initial temperature (70°C in the case of WEST) in less than 30 s after the pulse. For discharges #55 790 and #55 792, applying the same seeding rate, a remarkable reproducibility of both the D_2 and N_2 balance is observed. For the last pulse of the series

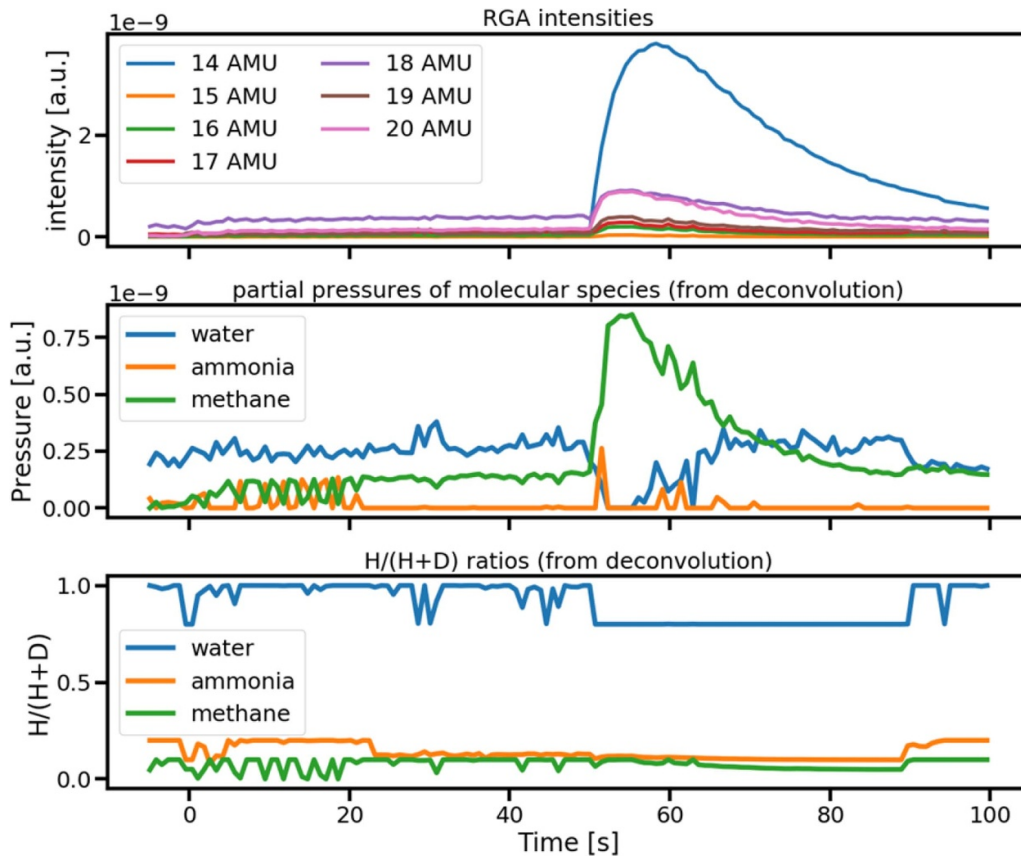


Figure 7. Time evolution of the mass 20 (ND_3 , CD_4 and D_2O) measured in the RGA for pulse #55792, which contained the most nitrogen. ND_3 was neither detected during the pulse (0–50 s) nor during the recovery and outgassing phase following the plasma discharge ($t > 50$ s).

(#55794), the larger N_2 recovery was largely due to the disruption during the heating phase when the plasma interacted strongly with the upper divertor. The amount of N_2 recovered after 25 min was on the scale of 3.0 Pa m^3 , corresponding to 70% of the amount injected (4.39 Pa m^3). For the seeded pulses, the amount of N_2 recovered 30 min after the end of the pulse is on the scale of 35% but higher values were possible after a disruption (see table 1). This also suggests that most of the N_2 was retained in the surfaces ‘facing’ the plasma.

Although the neutral pressures (total and partial) at the end of all these discharges are rather high, meaning that the signal to noise ratio exhibits favourable conditions, no ND_3 was detected at all in the RGA during the discharge or at the end of the discharge when the plasma recombined and during the 30 min of outgassing between pulses.

4. Discussion

Except for one pulse (#55790), N_2 was injected at the beginning of the plasma discharge (0–3 s) during the limiter phase (0–1 s) and the early X-point phase (1–3 s) through the midplane, and the effect of this injection on the plasma is different compared to the N_2 injection at the OSP region during the main heating phase. On the one hand, this amount, being in the range of $0.15\text{--}0.2 \text{ Pa m}^3$, is totally negligible compared to the 2.46

to 6.32 Pa m^3 injected during the X-point and heating phases. On the other hand, this early injection is readily detected by the RGA as neutrals at the edge plasma and in the confined plasma, as confirmed by both the N(V) and N(VII) signals, which exhibit a ‘peak’ at the beginning of the plasma. If no N_2 is injected during this early plasma phase, no N_2 is detected at all, even if N_2 has been seeded during the heating phase in the previous pulse. This is illustrated by pulse #55790 in figure 6 and this behaviour demonstrates that there is no legacy of the N_2 injected during the previous plasmas.

These results also support the fact that the N_2 reservoir is primarily located close to the OSP region where the N_2 is injected. Indeed, when compared to long discharges performed in the same conditions with N_2 injected through the midplane, N_2 was detected by the RGA during the plasma discharge, meaning that all this N_2 is not fully ionised and a part can be directly pumped by the main pumping system, as suggested in [10]. As a consequence, since no legacy is observed over this series of experiments, these measurements by the RGA support the fact that nearly no (totally negligible) N_2 is exhausted during the discharge and that a significant part ($\sim 35\%$) of the retained nitrogen over the discharge is released after the discharge.

For the four seeded discharges, the overall N balance exhibits a reservoir in the range of $\sim 6 \times 10^{21} \text{ N}$ ($\sim 65\%$ of the total N_2 injected). If we assume that the N sticks to the W wall, with a density on the scale of $1 \times 10^{19} \text{ Nm}^{-2}$, this supposes a flat W

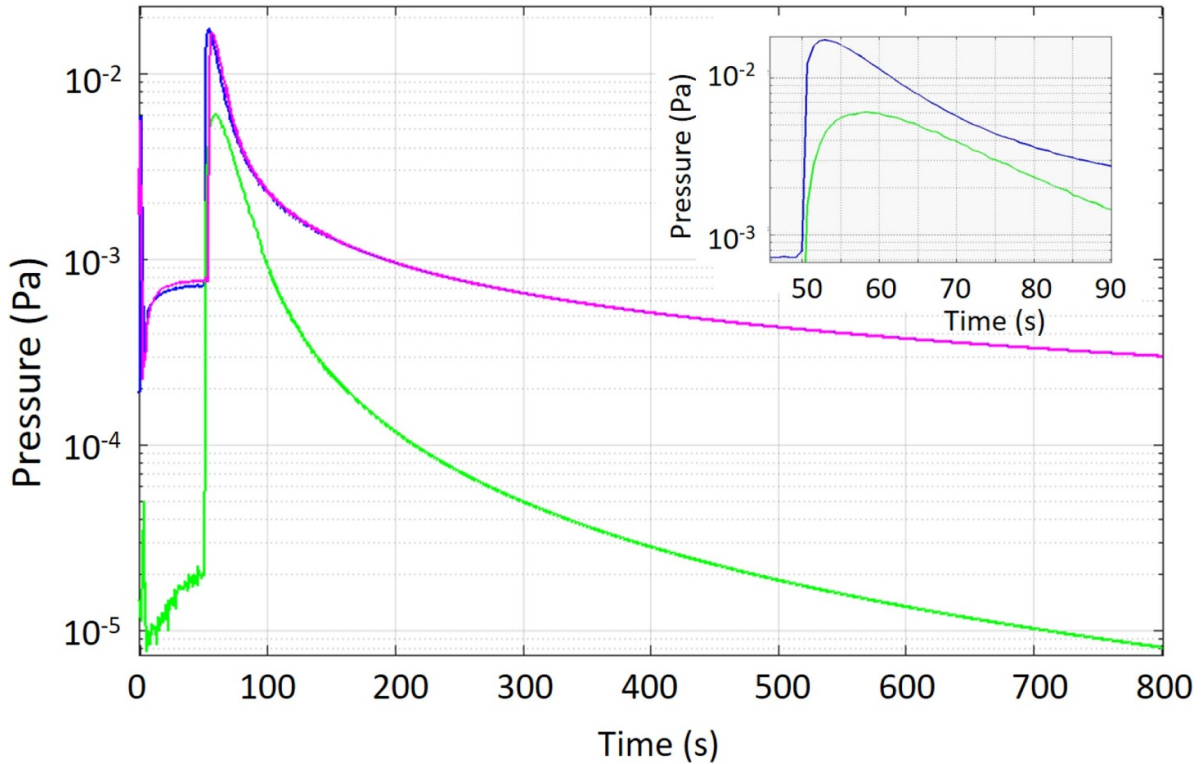


Figure 8. Time traces of the D_2 pressure for pulses #55 787 (m), #55 792 (b) and the partial pressure of N_2 (g) for the pulse #55 792. For the two pulses, the D_2 pressures are very close and behave in line with $t^{-0.7}$, whilst the N_2 (g) pressure has to be adjusted using a law $\propto t^{-1.6}$. The insert shows that for discharge #55 792, the maximum D_2 (b) pressure was reached at 53 s and the maximum N_2 pressure (g) was reached at 58 s.

surface of 600 m^2 which is not consistent with the $\sim 100 \text{ m}^2$ of the surface in view of the plasma ($\sim 20 \text{ m}^2$ for both the lower and upper W divertors and 80 m^2 for the stainless steel first wall). Considering the ion implantation and the neutral penetration in the bulk W, the retention can reach $2 \times 10^{20} \text{ Nm}^{-2}$ [12] with ion energies in the range from 250–500 eV. Such a retention could be obtained with surfaces of $\sim 30 \text{ m}^2$, which appears to be close to the exposed W surface of the upper divertor (10 m^2). However, the upper divertor is made of copper with a W coating of $15\text{--}20 \mu\text{m}$. The porosity of such a coating is larger than the W bulk contributing to the absence of saturation of the N reservoir.

In addition, since, the effects of boronisation can be observed (using O as the reference) over a maximum of $\sim 15\text{--}20$ pulses, this N_2 reservoir cannot be attributed to the boronisation performed more than 40 pulses before these experiments given that the O signal for all these experiments is in the same range as for the few discharges performed just prior to these N_2 experiments.

These results have to be compared to those obtained at JET-ILW [8] and AUG [9], which are equipped with non-actively-cooled divertor W coating targets. In the seeded L-mode experiments ($I_p/B_T = 2.0 \text{ MA}/2.2 \text{ T}$) reported for JET-ILW [8], the N_2 was injected into the divertor SOL through the toroidally symmetric gas injection ring (gas introduction module: GIM 9) in the vicinity of the horizontal W target plate (so-called ‘tile 6’) where the OSP was positioned. Injection rates between 1.4 and $5.4 \times 10^{21} \text{ e}^- \text{ s}^{-1}$ (respectively 0.2 and $0.77 \times 10^{21} \text{ N s}^{-1}$)

were applied for 4–5 s for ten discharges. A total amount of $3.62 \times 10^{22} \text{ N}$ was injected over the course of the ten discharges. This corresponds to a rate six to seven times higher than in WEST ($9.0 \times 10^{21} \text{ N}$) but for a shorter duration (4–5 s, compared to 40 s) whilst the injection location is very close to the gap entrance where the cryopump is installed. In these JET-ILW experiments, the gas balance measurements indicate a N_2 retention in the range of 50% (the same range as that observed in WEST) and also a significant increase in D_2 retention, compared to reference experiments. Whilst no effect of N_2 injection has been noticed at all on the D_2 balance in WEST, according to the author, this ‘extra’ D_2 retention in JET-ILW can be attributed to the N_2 seeding through ammonia formation corresponding to roughly 15% of the injected N atoms having been converted to ND_3 . This is a huge percentage which is not supported from the experiments reported from AUG and discussed below. In addition, in these L-mode experiments, no clear evidence of ND_3 formation was detected in the RGA located in the divertor region although a nitrogen–deuterium (ND) line was observed (at 336.0 nm) during plasma operations. The absence of clear measurements is attributed to the long distance from the ammonia formation to the RGA location, consistent with a production rate below the sensitivity of the RGA system between pulses.

In AUG, N_2 injection experiments were performed in an H-mode discharge with both ECRH and NBI heating, with an averaged plasma density of $7 \times 10^{19} \text{ m}^{-3}$, and a stable flat-top phase before the onset of nitrogen seeding [9]. The N_2

was injected into the private flux region, at a constant seeding rate of $1.7 \times 10^{21} \text{ N s}^{-1}$, adjusted to keep the outer divertor in an attached state. A total amount of $4.05 \times 10^{22} \text{ N}$ was injected over six discharges. In AUG, three RGAs were used for potential ND_3 detection, located in the inner divertor, the outer divertor and the midplane. In these experiments, evidence of ammonia formation was reported during the plasma operation, particularly in the inner divertor, as it was an order of magnitude higher than the impurity partial pressure in a non-seeded discharge. The amount corresponded to a 2% concentration in the neutral gas. This is very low compared to the 15% suggested in JET-ILW [8] which in the reported context (the ammonia amount evaluated from the N_2 and D_2 retention) seems strongly overestimated. However, during the plasma discharge, a huge difference appeared in the gas composition between the inner and outer divertors, dominated by ammonia and water, respectively. Although not discussed here, this could be linked to the detached conditions of the inner leg leading to a lower ionisation rate of the potential ND_3 formed in the vicinity of the inner strike point. The absolute value of the ammonia pressure was also 50 times higher in the inner sub-divertor region compared to the outer, whilst the N_2 pressure in the midplane remained very low and no sign of ammonia was detected during the plasma. In AUG, the authors report that while ammonia can be formed in surface reactions both on plasma-facing and plasma-shaded surfaces, it is only the ammonia formed on plasma-shaded surfaces that can make a significant contribution to the net ammonia production. The authors suggest that the ammonia formed in the divertor could not migrate to the midplane in the discharge phase, as it is promptly dissociated to N and D atoms in the plasma, thereby supporting the fact that no ammonia can be detected in the midplane before the end of the discharge. This appears to be somewhat contradictory to the results observed in WEST, where the upper divertor is open and where the absence of compression generated by a closed divertor (as is the case at both AUG and JET-ILW) appears to create favourable conditions for both the N_2 and the ND_3 formed to migrate up to the midplane. However, this means that a significant amount of ND_3 has to be formed prior to any migration compared to reionisation, which is not likely to be the case in WEST. Although the amount of N injected in WEST ($9.0 \times 10^{21} \text{ N}$) can appear low compared to JET-ILW and AUG with 3.62×10^{22} and $4.05 \times 10^{22} \text{ N}$ injected, respectively, it is worth remembering that the absence of N_2 pumping in WEST allows for all the N_2 injected to be dissociated (and therefore to potentially form ND_3). In both JET-ILW and AUG a non-negligible part (always very difficult to assess) of the injected N_2 is directly pumped by the cryo-pumping systems meaning that a direct comparison of the absolute amount of N injected is not the primary criteria.

For all three experiments (JET-ILW, AUG and WEST), the presence of ammonia formation resulting from N_2 injection is deduced through a model. Indeed, the mass spectrum of ammonia overlaps with methane and water, which are part of the neutral gas composition in the sub-divertor region and

the midplane during both the pulse and post-pulse phases. The same model, described in detail in [11], is used for the three reported experiments and allows for the proportion of each of the three gases to be evaluated. From the three experiments, the strong increase of ammonia deduced for AUG appears very convincing, given the ND_3 formation in the sub-divertor area, particularly when compared to the non-seeded case. However, it could be worth repeating these experiments with the N^{15} isotope allowing for single-mass monitoring and thereby preventing any discussion or doubt regarding the fits that have to be performed to resolve the overlaps of ammonia, water and methane in the analysis of the RGA data when using N^{14} .

Compared to the JET-ILW and AUG experiments, the results observed at WEST can lead to the following interpretation. Since there is no active pumping and no increase of the radiation is observed, the N_2 balance in the WEST experiments clearly shows that there is a reservoir of N_2 which is filled up during the plasma discharge, but without reaching saturation. This reservoir totally dominates the N_2 balance and as long as saturation is not reached, this could be the reason why no ammonia at all is detected throughout all these experiments (both in the plasma discharge and the outgassing phase). In other words, as long as this N_2 reservoir is not saturated, there is no (or not enough) N available for significant ND_3 formation. This is also complementary and consistent with the results obtained at both JET-ILW and AUG suggesting that ammonia formation only occurs in the vicinity of the sub-divertor region (recycling regions). This is also very likely the dominant location of the N_2 reservoir, since except in the divertor, no N_2 is detected in the midplane during plasma operations even in AUG. In JET-ILW the presence of ammonia was very weak and could be the signature of the non-saturation of the N_2 reservoir. In WEST, according to the N(VII) behaviour (figure 5), it is very clear that this reservoir is not saturated at all, thereby explaining a weak ND_3 production that cannot be detected. In AUG, in spite of the strong ammonia production in the inner divertor associated with a high N_2 injection compared to JET-ILW and WEST, it is worth noting that a few seconds after the pulse, the signature of ammonia disappears very quickly from the divertors (inner and outer) whilst it always remains very low in the midplane. The results obtained in the three devices are consistent with the potential saturation of the N_2 reservoir prior to potential significant ND_3 formation above the detection threshold. In WEST, although the particle flux is significantly lower than it will be in ITER, the edge T_e in the divertor region was in the same range as predicted for ITER. These plasma conditions in the vicinity of the strike points, as well as the constant surface temperature over these long durations due to actively cooled PFCs are relevant to what is expected in ITER.

Further experiments, with repetitive long discharges in a steady state, with a higher radiative fraction (most likely a semi-detached plasma) with constant N_2 seeding (N^{15} encouraged) would allow for clarification regarding the N_2 reservoir and its potential saturation leading to a threshold enhancing the corresponding rate of ND_3 formation and release.

5. Conclusions

A series of long and steady-state discharges has been performed in the USN configuration, with constant N₂ seeding from the OSP region totaling 237 s of plasma (~4 min). A total of 18.65 Pa m³ of N₂ was injected in four consecutive discharges through the OSP for up to 35 s and with an injection rate of 0.21 Pa m³ s⁻¹. For all these experiments with N₂ seeding, a very weak effect on the radiated power (edge and bulk) has been observed. In the absence of active pumping, at this injection rate, steady-state conditions are reached, showing that there is a constant retention of the N₂, while no saturation was observed for durations of around 35 s. The D₂ recovery 30 minutes after the end of these long discharges is in the range from 80%–85% which is consistent with what can be expected for metallic devices. Also, the D₂ retention and recovery does not appear to be influenced by the N₂ injection. The N₂ recovery during the 25–30 min following the pulse is in the region of 35% whereas it can reach up to 70% during a disruption. In the absence of active pumping, a saturation of the N₂ wall pumping over the seeded duration could have been expected. This has not been the case at all and since no legacy from the N₂ injection has been observed during the following pulse, this shows that the N₂ reservoir is not saturated.

Considering the N₂ balance over such long timescales and in the absence of active pumping in the USN configuration, these experiments suggest that the majority of the injected N₂ is retained in the the upper divertor made of copper with a W coating of 15–20 μm. The porosity of this coating is larger than the W bulk, thereby enhancing the volume of this N reservoir. As a consequence, since the saturation of this reservoir is not reached, this results in a very weak ND₃ production. Prior to this saturation, no (or not enough) N is available for ND₃ formation, explaining why no ND₃ at all is detected in the WEST experiments. Finally, this weak production is also consistent with a detection rate below the sensitivity of the RGA system between pulses.

The results obtained in the three devices (JET-ILW, AUG and WEST) are consistent with the saturation of the N₂ reservoir prior to the potential ND₃ formation. Ammonia has been detected in AUG, where the strongest N₂ injection has been performed, whilst in JET-ILW, the ammonia detection was close to the detection limit.

Further experiments with repetitive long discharges in a steady state, with a higher radiative fraction (most likely a semi-detached plasma) with constant N₂ seeding would allow for clarification regarding the potential N₂ reservoir and the corresponding rate of ND₃ formation and release. Once again, the absence of active pumping in the USN configuration coupled with the actively cooled PFCs in WEST appears to be beneficial for the estimation of the N₂ reservoir that needs to be saturated prior to significant ND₃ formation as observed in AUG.

Acknowledgments

This work has been carried out within the framework of the EUROfusion Consortium, and has received funding from the Euratom research and training programme 2014–2018 and 2019–2020 under Grant Agreement No. 63253. The views and opinions expressed herein do not necessarily reflect those of the European Commission or of the ITER Organization.

ORCID iDs

T. Dittmar  <https://orcid.org/0000-0002-4325-7979>

S. Brezinsek  <https://orcid.org/0000-0002-7213-3326>

References

- [1] ITER Organization 2018 ITER research plan within the staged approach ITER Technical Report ITR-18003 (<https://www.iter.org/technical-reports>)
- [2] Pitts R. *et al* 2019 *Nucl. Mater. Energy* **20** 100696
- [3] Kallenbach A. *et al* 2013 *Plasma Phys. Control. Fusion* **55** 124041
- [4] Giroud C. *et al* 2017 *Plasma Phys. Control. Fusion* **57** 035004
- [5] Walker R. and Gilbert M.R. 2017 *Fusion Eng. Design* **124** 892–5
- [6] Bucalossi J. *et al* 2014 *Fusion Eng. Design* **89** 907–12
- [7] Bourdelle C. *et al* 2015 *Nucl. Fusion* **55** 063017
- [8] Oberkopfer M. *et al* 2013 *J. Nucl. Mater.* **438** S258–61
- [9] Drenik A. *et al* 2019 *Nucl. Fusion* **59** 046010
- [10] Dittmar T. *et al* 2020 *Phys. Scr.* **T171** 014074
- [11] Neuwirth D. *et al* 2012 *Plasma Phys. Control. Fusion* **54** 085008
- [12] Meisl G. *et al* 2014 *New J. Phys.* **16** 093018